Published online 25 May 2016

Nucleic Acids Research, 2016, Vol. 44, No. 16 ***7659–7672***
doi: 10.1093/nar/gkw463

EZH2 is required for mouse oocyte meiotic maturation by interacting with and stabilizing spindle assembly checkpoint protein BubRI

Yi Qu, Danyu Lu, Hao Jiang, Xiaochun Chi and Hongquan Zhang*

Department of Human Anatomy, Histology and Embryology, Key Laboratory of Carcinogenesis and Translational Research, Ministry of Education, and State Key Laboratory of Natural and Biomimetic Drugs, Peking University Health Science Center, Beijing 100191, China

Received January 21, 2016; Revised May 15, 2016; Accepted May 17, 2016

ABSTRACT

Enhancer of zeste homolog 2 (EZH2) trimethylates histone H3 Lys 27 and plays key roles in a variety of biological processes. Stability of spindle assembly checkpoint protein BubR1 is essential for mitosis in somatic cells and for meiosis in oocytes. However, the role of EZH2 in oocyte meiotic maturation was unknown. Here, we presented a mechanism underlying EZH2 control of BubR1 stability in the meiosis of mouse oocytes. We identified a methyltransferase activity-independent function of EZH2 by demonstrating that EZH2 regulates spindle assembly and the polar body I extrusion. EZH2 was increased with the oocyte progression from GVBD to MII, while EZH2 was concentrated on the chromosomes. Interestingly, inhibition of EZH2 methyltranferase activity by DZNep or GSK343 did not affect oocyte meiotic maturation. However, depletion of EZH2 by morpholino led to chromosome misalignment and abnormal spindle assembly. Furthermore, ectopic expression of EZH2 led to oocyte meiotic maturation arrested at the MI stage followed by chromosome misalignment and aneuploidy. Mechanistically, EZH2 directly interacted with and stabilized BubR1, an effect driving EZH2 into the concert of meiosis regulation. Collectively, we provided a paradigm that EZH2 is required for mouse oocyte meiotic maturation.

INTRODUCTION

Polycomb group proteins are transcriptional repressors that are involved in epigenetic regulation of gene expression during development (1). Enhancer of zeste homologue 2 (EZH2), as a core member of PRC2 (polycomb repressive complex 2), is directly involved in the trimethylation of lysine 27 on histone H3 through its SET (suppressor of variegation, enhancer of zeste and trithorax) domain, which is the catalytic subunit of PRC2 (2). EZH2 has been known to play key roles in X-chromosome inactivation and embryonic development. EZH2-deficient embryos displayed impaired growth potential, preventing development of embryonic stem cells and the onset of differentiation of trophectoderm cells (3–5). In the early mouse embryo development, EZH2 was detected as a maternally inherited protein in the oocytes (3,5). Lack of maternal EZH2 resulted in severe growth retardation of neonates (3), suggesting the importance of EZH2 in the control of female reproduction. Maturation of oocytes is one of the key step in female reproduction. Thereby it is tempting to understand whether EZH2 plays a role in the regulation of oocyte meiotic maturation.

In meiosis, two successive divisions happen with only one round of DNA replication (6). Missegregations during meiotic divisions can cause aneuploidy (7). Fertilization of aneuploid oocytes in human led to spontaneous abortions during the first trimester, and if survival occurs to term, will result in aneuploid embryos (8). One of the most common viable aneuploidy is trisomy 21 on account of the missegregation of chromosome 21 in female meiosis I (9). Accurate control of microtubules organizing into the barrel-shaped bipolar spindle, with all the chromosomes aligned at the spindle equator, is required for orderly meiosis during oocyte maturation (10). Errors at this step could lead to the generation of aneuploid oocyte.

Through spindle assembly checkpoint (SAC) driven mechanisms meiosis could enter anaphase when all chromosomes are successfully attached to the bipolar spindle (11). Unattached kinetochores can inhibit the activation of the anaphase promoting complex/cyclosome (APC/C), an E3 ubiquitin ligase (12). When the SAC pathway is shut down, APC/C ubiquitinates securin and cyclin B, leading to their degradation and resulting in anaphase onset (13). BubR1 is an important SAC protein. Recent studies have identified that overexpression of BubR1 caused meiosis arrest and depletion of BubR1 led to acceleration of the first meiosis progression (14). Furthermore, BubR1 was found

*To whom correspondence should be addressed. Tel: +86 10 8280 2424; Fax: +86 10 8280 2424; Email: Hongquan.Zhang@bjmu.edu.cn

not required for maintaining GV arrest in oocytes but necessary for the establishment of stable spindles (15). Choi *et al*. reported that BubR1 is acetylated by the histone acetyltransferase PCAF at K250, leading to resistance of BubR1 degradation by APC/C-Cdc20-mediated pathway (16).

In the present study we reported a link between EZH2 and oocyte meiotic maturation regulation in mice. We demonstrated that EZH2 is indispensable in the control of chromosome alignment and euploidy in mouse oocytes, mechanistically linking EZH2 to the SAC protein, BubR1. Further, we pinpointed that EZH2 coordinates with BubR1 and p300/CBP associated factor (PCAF) to regulate mouse oocyte meiotic maturation through forming a molecular complex encompassing EZH2, BubR1 and PCAF, a previously unidentified mechanism underlying meiosis in oocytes.

MATERIALS AND METHODS

Mice

Three-week-old female ICR mice were used in this study. Animal care and handling were conducted in accordance with the Institutional Animal Welfare and Ethics Committee of Peking University (No. LA2011-73).

Antibodies

Rabbit polyclonal anti-EZH2, rabbit polyclonal anti-PCAF were purchased from Cell Signaling Technology (Beverly, MA, USA); goat polyclonal anti-BubR1, rabbit polyclonal anti-H3K27me3 and rabbit polyclonal anti-α-tubulin were purchased from Abcam (Cambridge, MA, USA); human CREST antibody was purchased from Fitzgerald; and rabbit polyclonal anti-Myc was purchased from MBL (Nagoya, Japan). Alexa Fluor 488 donkey anti-rabbit IgG (H + L), Alexa Fluor 568 donkey anti-goat IgG (H + L) were purchased from Invitrogen (Eugene, OR, USA); and CY5-conjugated goat anti-human IgG was purchased from Jackson ImmunoResearch.

Oocyte collection and culture

After mice were superovulated by intraperitoneal injection with 5 IU pregnant mare serum gonadotropin (PMSG) for 48 h, large antral follicles were punctured under a stereoscopic microscope (320 773; Olympus, Tokyo, Japan) to release GV oocytes. The oocytes were cultured in M2 medium under mineral oil at 37°C with 5% in a CO_2 incubator and collected at different times for different experiments.

EZH2 expression vector construction and mRNA synthesis

Myc-EZH2 expression plasmids were constructed by subcloning the EZH2 cDNA fragments into the pCS2+ vector. The full length EZH2 sequence was cloned by polymerase chain reaction (PCR) with the following primers: forward primer, 5′-ATATGGCCGGCCAATGGGCCAGACTGGG-3′, and reverse primer, 5′-GGCGGCGCGCCTCAAGGGATTTCCATTT-3′. The EZH2 (1-609) sequence was cloned by PCR with the following primers: forward primer, 5′-TATGGCCGGCCAATGGGCCAGACTGGG-3′, and reverse primer, 5′- TTGGCGCGCCGCCCCGCTGAATACT-3′. And the SET domain (610-746) of EZH2 sequence was cloned by PCR with the following primers: 5′- TATGGCCGGCCAGGCTCCAAAAAGCATC-3′, and reverse primer, 5′- TTGGCGCGCCTCAAGGGATTTCCATTTCT-3′. All of these PCR products were purified, and then cloned into pCS2+ vector.

The Myc-EZH2-pCS2+ plasmids were linearized and purified by gel extraction kit (Qiagen, Düsseldorf, Germany). SP6 mMessage mMachine (Ambion, Austin, TX, USA) were used to obtain capped mRNA and then the mRNA were recovered by Phenol: chloroform extraction and isopropanol precipitation.

EZH2 knockdown and overexpression

EZH2 morpholino, rabbit polyclonal anti-EZH2 or Myc-EZH2 mRNA was microinjected into oocytes by a Nikon Microinjector (TE2000-U, Nikon, Tokyo, Japan).

For knockdown experiment, 1 mM EZH2 morpholino antisense oligos (Gene Tools, Philomath, OR, USA, 5′-ATTTCTTCCCAGTCTGGCCCATGAT-3′) were microinjected into the GV oocyte cytoplasm. The MO standard control (5′-CCTCTTACCTCAGTTACAATTTATA-3′) was injected. After injection, the oocytes were cultured for 24 h in M2 medium containing 2.5 μM milrinone to facilitate knockdown of EZH2.

For EZH2 antibody injection, the same method was adopted as above, except that the antibody was injected into cytoplasm at Pro-Met I stage and after injection the oocytes were cultured in M2 medium directly. The same amount of phosphate buffered saline (PBS) was injected as control.

For overexpression experiments, about 5–10 pl Myc–EZH2 mRNA in RNase-free PBS solution (2.5 mg/ml) was injected into cytoplasm of GV oocytes. The same amount of Myc mRNA in RNase-free PBS was injected as control. Oocytes were arrested at the GV stage in M2 medium containing 2.5 μM milrinone for 3 h and then released in M2 culture medium.

Real-time quantitative PCR analysis

Total RNA was extracted from 30 oocytes using RNeasy micro kit (Qiagen, Düsseldorf, Germany), and the cDNA was generated with Sensiscript RT Kit (Qiagen, Düsseldorf, Germany). The cDNA was added to a qPCR mixture that contained 2× SYBR Green PCR master mixes (Roche, Indianapolis, IN, USA) and 10 μM following primers: the forward primer of EZH2 is 5′-CAGATAAGGGCACCGCAGAA-3′, and the reverse primer is 5′- ACATTCAGGAGGCAGAGCAC-3′. Assays were performed in triplicate. The PCR steps included incubations for 10 min 95°C, followed by 40 cycles, with each cycle consisting of 15 s at 95°C and 1 min at 60°C.

Western blot analysis

Oocytes were collected in Laemmli sample buffer and heated for 5 min at 100°C. Samples were separated by 8% sodium dodecyl sulphate-polyacrylamide gel electrophoresis (SDS-PAGE) and transferred to polyvinylidene fluoride

membranes. The resultant membranes were restrained with 5% (w/ml) fat-free dry milk/Tris buffered saline-Tween 20 (TBST) at room temperature for 1 h, and then incubated at 4°C overnight with primary antibodies as follows: rabbit anti-EZH2 antibody (1: 1000), goat anti-BubR1 antibody (1: 1000), rabbit anti-Myc antibody (1: 1000), rabbit anti-PCAF antibody (1: 1000) and rabbit anti-α-tubulin (1: 2000) as control. After three 10 min wash in TBST, the membrane was incubated with its corresponding secondary antibody for 1 h at room temperature. Immobilized antibodies were detected by enhanced chemoluminescence (Pierce Chemical Co, Rockford, IL, USA).

Immunofluorescent analysis

Oocytes were fixed with 4% paraformaldehyde for at least 30 min, followed by permeabilization with 0.5% Triton X-100 at room temperature for 30 min, blocked in 1% bovine serum albumin-supplemented PBS for 1 h and then incubated overnight at 4°C with primary antibodies as follows: rabbit anti-EZH2 antibody (1:50), human CREST antibody (1:40), goat anti-BubR1 antibody (1:50), rabbit anti-Myc antibody (1:50), rabbit anti-H3K27me3 antibody (1:50) and rabbit anti-α-tubulin (1:50). After three washes in PBS, the oocytes were labeled with Alexa Fluor 488 donkey anti-rabbit IgG, Alexa Fluor 568 donkey anti-goat IgG and CY5-conjugated goat anti-human IgG (1:200) for 1 h at room temperature, and then washed three times with PBS. Chromosomes were evaluated by staining with propidium iodide (PI; red, 10 μg/ml) for 10 min or Hoechst 33342 (blue, 5 μg/ml) for 20 min. Then the immunofluorescent images were captured by a confocal laser-scanning microscope (Carl Zeiss LSM780, Germany).

Inhibitor treatments

DZNep (Millipore, Billerica, MA, USA) stock solution was diluted to 50 mM in dimethyl sulfoxide (DMSO) and further diluted in M2 medium to a final concentration of 5 μM. GSK343 (Selleck, Billerica, MA, USA) stock solution was diluted to 10 mM in DMSO and further diluted in M2 medium to a final concentration of 1 μM.

Chromosome spreading assay

MII oocytes were treated with 1% sodium citrate for 15 min, and transferred to a glass slide one by one. Methanol: glacial acetic acid (3:1) was used to fix the oocyte. After the chromosomes were stained with PI (10 mg/ml), the specimen was examined with a confocal laser-scanning microscope (Carl Zeiss LSM780, Germany).

Co-immunoprecipitation and two-step co-immunoprecipitation

Approximately 2000 mouse oocytes were collected to accomplish co-immunoprecipitation experiments. All procedures followed the instructions of the Pierce co-immunoprecipitation Kit (Thermo Scientific, Rockford, IL, USA) or performed with relevant antibody and rabbit/goat immunoglobin-G which followed by incubating with protein A/G-Sepharose at 4°C overnight, and then the protein were subjected to SDS-PAGE and immunoblot analysis with the antibodies. The antibodies used for immuoprecipitation assays were rabbit anti-EZH2 antibody, rabbit anti-PCAF antibody and goat anti-BubR1 antibody.

For two-step IP, the first IP was performed with Flag-M2 beads or with mouse IgG, followed by incubating with protein G-Sepharose at 4°C for 4 h. After the beads were washed four times, the bound proteins were eluted with 3×FLAG peptide (250 mg/ml, Sigma). Then, the eluates were processed for the second IP with PCAF antibody or rabbit immunoglobin-G, followed by incubating with protein G-Sepharose at 4°C overnight. After the beads were washed three times, the eluates of protein samples from each step were subjected to western blot analysis (17).

GST pull-down assay

To obtain the GST-fusion proteins of EZH2, the sequence for the N-terminal (1–522), Cys-Rich (523–609) and SET (610–746) domains were amplified by PCR and subcloned into pGEX-4T-1 vector. GST and GST fusion proteins were expressed in *Escherichia coli* BL_{21} and purified with Glutathione Sepharose 4B beads (Pharmacia Biotech). The cell lysates of NIH3T3 were pre-cleared with Glutathione Sepharose 4B beads and GST. And then the lysates were incubated with beads containing GST fusion proteins at 4°C overnight. After being washed for four times, the target proteins were detected by Western blot analysis.

The amino acid sequences of BubR1 (1–700) and (701–1052) were amplified by PCR with the following primers: forward primer of BubR1 (1–700):GGGGTACCA ATGG CGGCGGT; reverse primer of BubR1 (1–700): CCGGGA TCCATCCTCATTACCTAATTCAA; forward primer of BubR1 (701–1052): GGGGTACCCGATTACTGCATTA AAC; reverse primer of BubR1 (701–1052): CGGGAT CCTCACTGAAAGAGCAA, and then subcloned into p3×FLAG-CMV^{TM}-10 expression vector. NIH3T3 cells were used for gene transfection. Gene transfections were performed using Lipofectamine 2000 (Invitrogen) according to the manufacturer's instruction. Cells were lysed with NP-40 buffer and then cell lysates were performed for co-immunoprecipitation with FLAG-M2 beads overnight at 4°C. After being washed for four times, the co-immunoprecipitated proteins were detected by western blot analysis.

Statistical analysis

The data are shown as mean ±SEM of results from three independent experiments, and $P < 0.05$ was considered statistically significant. Differences between groups were evaluated by one-way ANOVA or *t*-test.

RESULTS

EZH2 is increased during the oocyte meiotic maturation from stages GVBD to MII in mice

EZH2 is an important epigenetic regulator for a variety of biological processes including early embryogenesis, cell stemness and cancer progression. However, no indication

has been shown for EZH2 engagement in the regulation of oocyte maturation. To this end, we set out to examine whether EZH2 plays a role in oocyte maturation in a mouse model. We tried to answer first that whether EZH2 exists in mouse oocytes. Oocytes at different stages of oocyte meiotic maturation were collected from mice after PMSG treatment, and then were stained for EZH2 expression. Results showed that EZH2 is localized and enriched on the chromosomes at the GV and GVBD stages. Along with the maturation process of oocytes from GVBD to MII stages EZH2 spread out into the cytoplasm (Figure 1A), accompanied by an indication that EZH2 protein levels gradually raised during the progression of oocyte *in vitro* maturation. Furthermore, we collected 150 oocytes at each meiotic stage to examine the EZH2 protein level by Western blot analysis. Results demonstrated that EZH2 protein exists throughout the whole meiosis (Figure 1B). Interestingly, EZH2 protein showed a moderate level initially at GV stage, but gradually increased from GVBD to MII stages with a peak at MII (Figure 1B). EZH2 mRNA expression profile at the corresponding stages was also examined and results showed an almost identical trend as that of the protein levels (Figure 1C). Thus, the increase in EZH2 during maturation may also reflect a requirement for EZH2 following fertilization or early development.

Lack of EZH2 causes chromosome misalignment, abnormal spindles, aneuploidy and accelerated PB1 extrusion

Given that EZH2 may play an important role during oocyte maturation we continued to investigate the function of EZH2 in oocyte meiosis. To this end, control or EZH2 morpholino (MO-Control/MO-EZH2) was microinjected separately into the MII stage oocytes for testing the depletion efficacy of morpholino. We showed that there was a reduction in the protein level of EZH2 after MO-EZH2 morpholino treatment in western blot analysis (Figure 2A). After depletion of EZH2, the expression of H3K27me3 and H3K9me2 were greatly inhibited in the oocytes (Supplementary Figure S1). For formal experiments, the microinjected oocytes were allowed to arrest at the GV stage in milrinone-containing (2.5 μM) M2 medium for 24 h and then transferred to free-M2 medium for 14 h. Interestingly, during the maturation process of oocytes, we found that the PB1 extrusion rate of oocytes that reached MII in the EZH2 morpholino-microinjected group was higher than the control group at time points 9, 10 and 11 h (MO-Control, 9 h: 5.7%, 10 h: 22.8%, 11 h: 48.5%, $n = 92$; MO-EZH2, 9 h: 16.2%, 10 h: 39.3%, 11 h: 56.5%, $n = 86$). At time point 10 h difference between the MO-Control and MO-EZH2 groups was statistically significant (Figure 2B lower). However, difference of the two groups for the percentage of GVBD was not significant (Figure 2B upper). This result demonstrated that inadequate amount of EZH2 promotes the first polar body (PB1) extrusion. Given that EZH2 colocalizes with chromosomes, we therefore depleted EZH2 in oocytes of MI/MII stages by morpholino and stained them by an α-tubulin antibody and PI. After immunofluorescent staining the MI plate was measured and found it wider at MI stage in EZH2-depleted oocytes than the control ones (MO-Control: $n = 34$, MO-EZH2: $n = 49$, $P < 0.001$) (Figure 2C and D). To examine whether EZH2 may also associate with K-MT attachments we performed a cold treatment for oocytes (18). After the MI oocytes were transferred to M2 medium which was pre-cooled at 4°C for 10 min, most of the spindle microtubules remained intact with the kinetochores in the control group. While some of spindles disappeared in the EZH2 depleted oocytes and a significant number of chromosomes showed no attachments to microtubules (Figure 2E, and a series of z-slices in Supplementary Figure S2). These data indicated that loss of EZH2 causes a failure to maintain stable K-MT attachments. Likewise, by immunofluorescent staining we identified some types of chromosome defects in the MII MO-EZH2 oocytes (Figure 2F). The ratio of misaligned chromosomes in MO-EZH2 microinjected group was found much higher than that of the control group (MO-Control: 32.4 ± 4.0%, $n = 82$; MO-EZH2: 63.4 ± 5.8%, $n = 100$, $P < 0.01$) (Figure 2G). In addition, we also applied EZH2 antibody to block EZH2 function. We microinjected EZH2 antibody into the pro-Met I oocytes, a stage that displays higher EZH2 protein level as shown in Figure 1B. Interestingly, by blocking EZH2 by specific antibody at pro-Met I stage spindle collapse was observed, suggesting that EZH2 is required for spindle bipolarity (Supplementary Figure S3). To determine whether the abnormal spindle and misaligned chromosomes in MO-EZH2 oocytes may generate oocytes with aneuploidy, we therefore used chromosome spreading assay to examine the karyotype of MII oocytes. We found that most of the MO-EZH2 oocytes displayed incorrect numbers of chromosomes (Figure 2H and I, MO-Control: 14.8 ±0.4%, $n = 14$; MO-EZH2: 40.7 ± 2.2%, $n = 13$, $P < 0.01$), providing convincing evidence for aneuploidy induction. Taken together, these findings demonstrated that inadequate EZH2 could lead to an aberrant oocyte development.

Increased level of EZH2 leads to chromosome misalignment, aneuploidy and impaired PB1 extrusion

Aforementioned findings showed that depletion of EZH2 in oocytes causes abnormal meiosis, and then we asked whether increased EZH2 protein may affect the maturation of oocyte. To answer this question, full-length EZH2 mRNA with c-myc tag was *in vitro* transcribed from plasmid pCS2+ and then transcribed mRNA was microinjected into oocytes in GV stage. After culture for 6 h with the presence of 2.5 μM milrinone, the translated Myc-EZH2 protein was examined by western blot analysis with a Myc antibody. Result indicated that Myc-EZH2 protein was successfully produced in oocytes (Figure 3A). For formal experiment, oocytes with mRNA-EZH2 microinjected were incubated in milrinone-free M2 medium for 14 h. We found that the percentage of oocytes with mRNA-EZH2 microinjection displaying decreased PB1 extrusion than that of the mRNA-Control microinjected oocytes (Figure 3B left, mRNA-Control: 71.3 ± 9.4%, $n = 105$; mRNA-EZH2: 29.7 ± 2.2%, $n = 143$, $P < 0.01$) and the ratio of failure to extrude a PB was higher in the mRNA-EZH2 group than the mRNA-Control group (Figure 3B right, mRNA-Control: 18.5 ± 1.7%, $n = 63$; mRNA-EZH2: 40.2 ± 3.2%, $n = 96$, $P < 0.05$), strongly indicating that raised protein level of

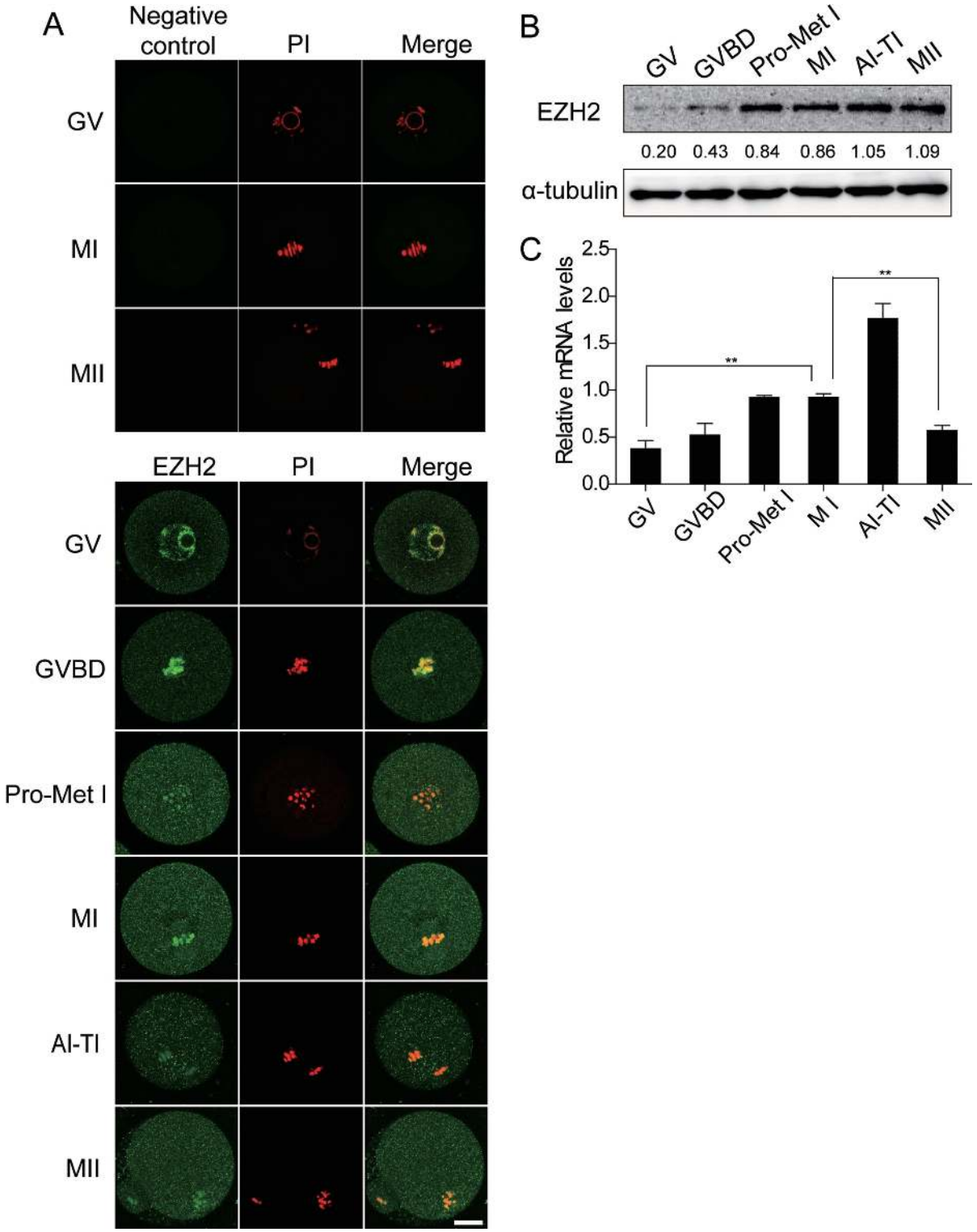

Figure 1. EZH2 protein level increases with the progression of mouse oocyte meiotic maturation. (**A**) EZH2 is redistributed in chromosomes during oocyte meiotic maturation. Oocytes from mice at different stages of meiotic maturation were stained with an EZH2 antibody (green) and Myc mRNA acted as negative control. DNA of chromosomes was stained with PI (Propidium iodide, red). Images were obtained by using a confocal microscope. EZH2 positive signals were observed mainly on the chromosomes at stages of GV and GVBD. Cytoplasmic staining for EZH2 was observed at stages of Pro-Met I to MII. Scale bar = 20 μm. (**B**) EZH2 protein levels at different stages of oocyte meiotic maturation were examined by western blot analysis using an EZH2 antibody with α-tubulin as a loading control. EZH2 amount at each stage from a representative experiment was quantified and displayed as indicated. (**C**) EZH2 mRNA levels were measured by qPCR. Data were normalized to the abundance of internal control GAPDH. Data are shown as mean ± SEM from three independent experiments, $P < 0.05$.

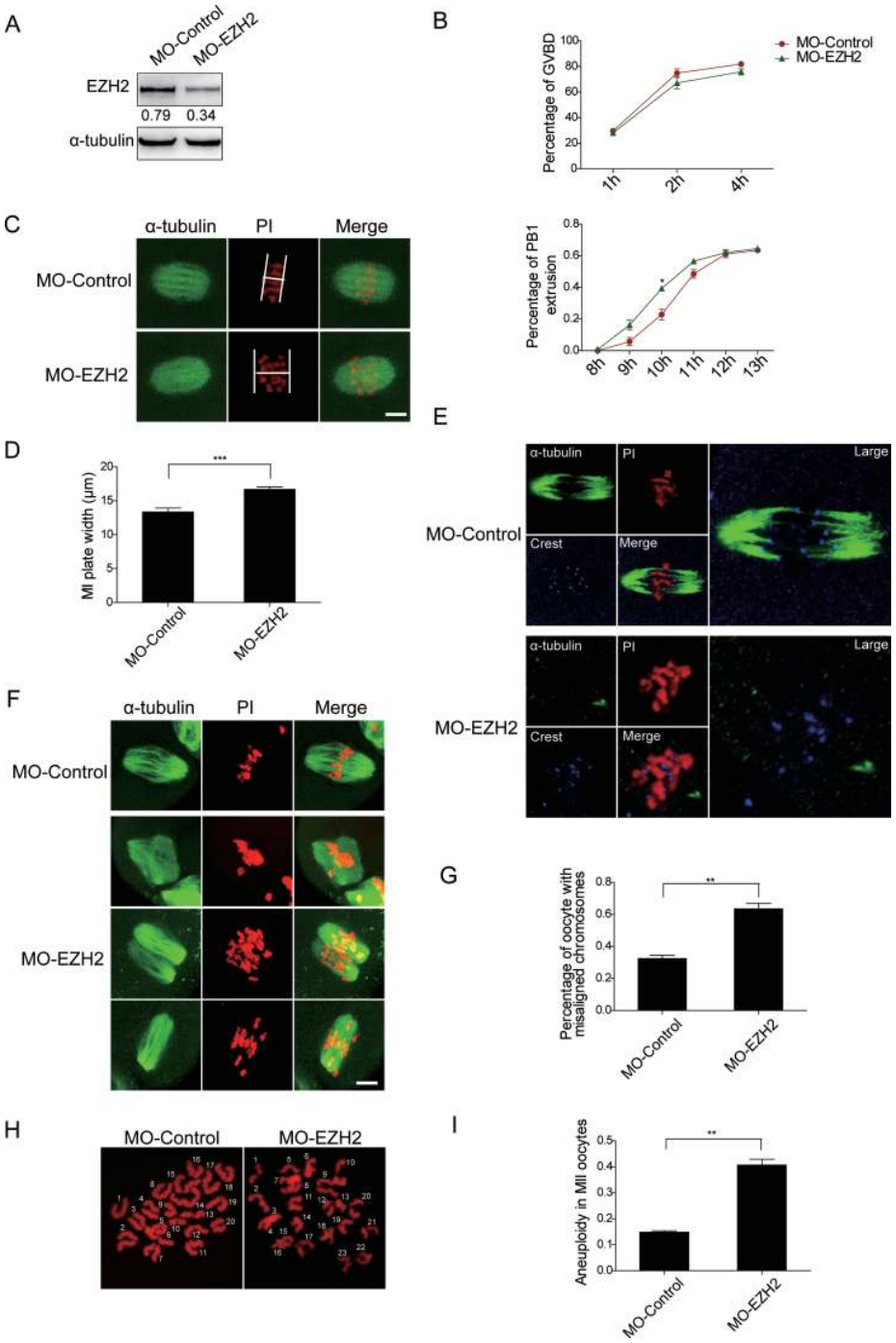

Figure 2. Depletion of EZH2 leads to chromosome misalignment, aneuploidy and acceleration of mouse oocyte meiotic maturation. (**A**) Mouse oocytes were arrested at the GV stage for 24 h, endogenous EZH2 in these oocytes was depleted by morpholino. Depletion of EZH2 was determined by western blot analysis using an EZH2 antibody. (**B**) GVBD rates and PB1extrusion rates between the control and EZH2 depletion groups were determined separately. Data were presented as mean ± SEM from three independent experiments. Upper: GVBD evolution rate was not significantly changed, $P > 0.05$. Lower: PB1 extrusion rate was obviously accelerated in EZH2 depletion group, $P < 0.05$. (**C** and **D**) Raised level of EZH2 in oocytes leads to wider MI plate and longer spindles (**C**). Oocytes microinjected with MO-EZH2 at MI were measured for the width of plates. Spindle was stained with an α-tubulin antibody (green) and DNA was stained with PI (Propidium Iodide, red). Scale bar = 4 μm. The width of MI plates was quantified in the control and EZH2 depletion oocytes (D). Data were expressed as mean ± SEM from three independent experiments, $P < 0.001$. (**E**) Oocytes were microinjected with MO-Control/MO-EZH2 and treated for 10 min at 4°C, followed by immunofluorescent staining. Green: α-tubulin; blue: crest; red: DNA. (**F**) Oocytes microinjected with the control-MO displayed normal spindle and MII plate (upper panel). Oocytes microinjected with the MO-EZH2 led to multipolar spindle (panel 2), two spindles (panel 3) and a wider MII plate with the chromosome displayed throughout the whole spindle (Panel 4). Green: α-tubulin; red: DNA. Scale bar = 4 μm. (**G**) Percentage of oocytes with chromosome misalignment in the MO-EZH2 microinjected group and MO-Control. Data were presented as mean ± SEM from three independent experiments, $P < 0.01$. (**H**) Chromosome spread in control and MO-EZH2 MII oocytes. Representative fluorescence images of euploid and aneuploid oocytes were shown. (**I**) Percentage of aneuploidy in control and MO-EZH2 oocytes was quantified. Data were expressed as mean ± SEM from three independent experiments, $P < 0.001$.

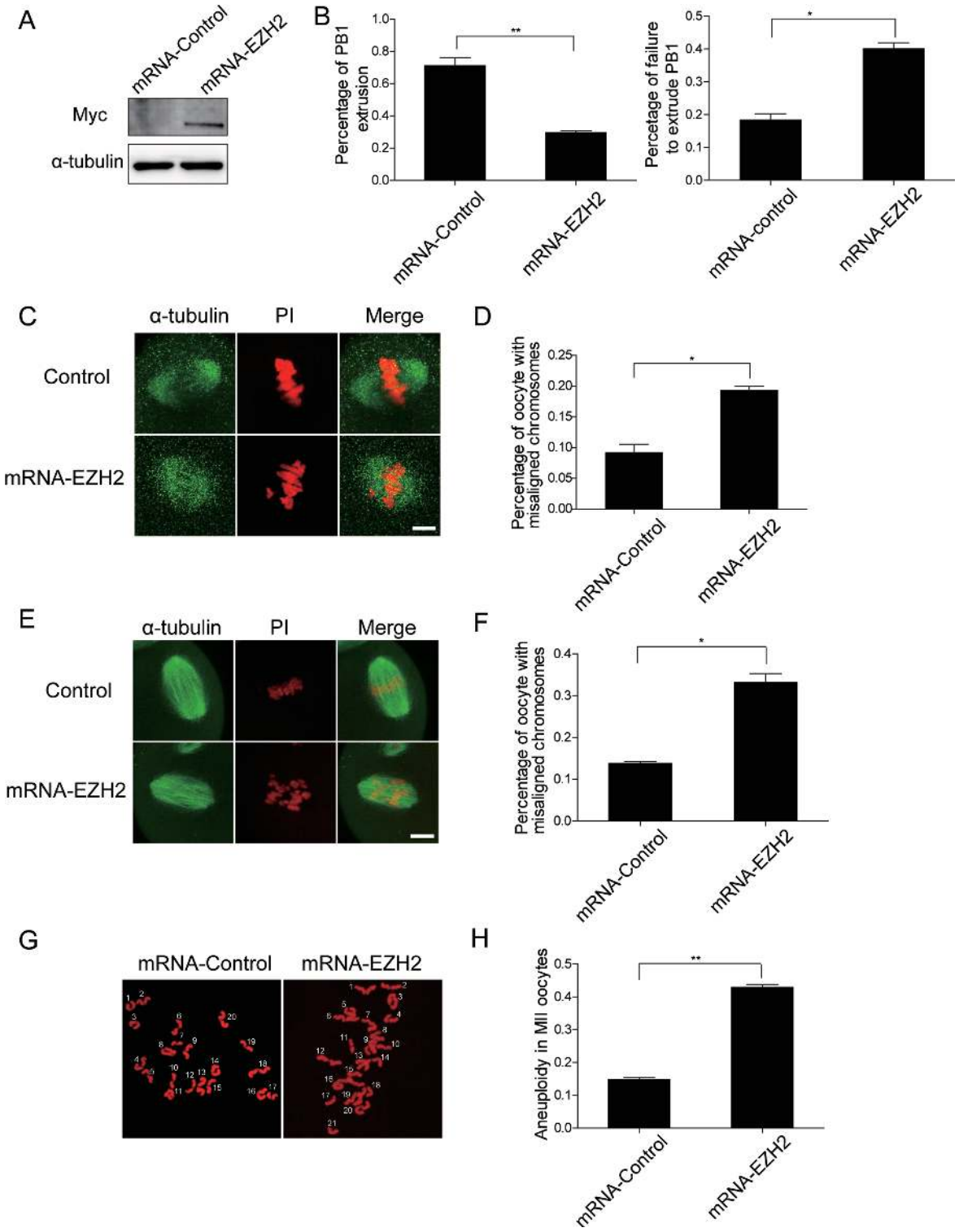

Figure 3. Raised level of EZH2 in oocytes leads to chromosome misalignment and aneuploidy. (**A**) The control and Myc-EZH2 mRNAs were *invitro* translated separately and western blot analysis was applied to confirm the translation of Myc-EZH2 in a cell-free *invitro* translational system with a Myc antibody. (**B**) PB1extrusion rates and the percentage of failure to extrude a PB between the control and mRNA-EZH2 groups were determined separately. Data were presented as mean ± SEM from three independent experiments. Left: Raised level of EZH2 in oocytes impairs the PB1 extrusion, $P < 0.01$. Right: the percentage of failure to extrude a PB was obviously increased in EZH2 depletion group, $P < 0.05$. (**C**–**F**) Raised level of EZH2 in oocytes causes chromosome misalignment. Oocytes were microinjected with the control or Myc-EZH2 mRNA and chromosome misalignment was detected at MI (C) and MII (E) stages. Green: α-tubulin; red: DNA. Scale bar = 4 μm. Percentage of oocytes with chromosome misalignment at stages MI (D) and MII (F) was quantified. Data were expressed as mean ± SEM from three independent experiments, $P < 0.001$. (**G** and **H**) Raised level of EZH2 in oocytes leads to aneuploidy. Chromosome spreading was performed in oocytes microinjected with the control or Myc-EZH2 mRNA and aneuploidy was seen (G). Percentage of aneuploidy occurrence was quantified (H). Data were expressed as mean ± SEM from three independent experiments, $P < 0.001$.

EZH2 leads to an impaired oocytes meiotic maturation. In addition, we observed alterations of spindle shape and chromosome alignment under changing of the EZH2 level in oocytes. At the MI stage, oocytes with mRNA-EZH2 microinjected displayed collapse of spindle and chromosome misalignment (Figure 3C), which were quantified as shown in Figure 3D (mRNA-Control: 9.3 ± 1.3%, $n = 25$; mRNA-EZH2: 19.4 ± 0.7%, $n = 53$, $P < 0.05$). Likewise, for oocytes in MII stage a large proportion of oocytes displayed misaligned chromosomes under increased level of EZH2 (Figure 3E), which were quantified as shown Figure 3F (mRNA-Control: 13.8 ± 1.0%, $n = 36$; mRNA-EZH2: 33.3 ± 2.1%, $n = 42$, $P < 0.05$). However, when we overexpressed EZH2 we did not find an obvious change in the levels of H3K27 me3 and H3K9me2, even though the chromosome arrangement has been disordered (Supplementary Figure S4). Furthermore, karyotype analyses showed a plenty of MII oocytes with aneuploidy by increased level of EZH2 (Figure 3G), which were quantified as shown in Figure 3H (mRNA-Control: 14.8 ±0.6%, $n = 13$; mRNA-EZH2: 42.3 ± 1.5%, $n = 16$, $P < 0.01$). These data suggested that raised EZH2 in oocytes at different stages affects oocyte maturation. In short, the amount of EZH2 in oocytes is critical for mouse oocyte meiotic maturation.

EZH2 methyltranferase activity is not required for oocyte meiotic maturation

Given that EZH2 is a methyltransferase and mediates H3K27 trimethylation (2), we therefore interested in answering whether EZH2 regulation on mouse meiotic maturation depends on its methyltransferase activity. To this end, we treated the oocytes with DZNep and GSK343, two potent EZH2 inhibitors. Both of them have been reported not to effect the expression of EZH2 under low concentration (19–21). We tested that 5 μM DZNep and 1μM GSK343 do not affect the protein level of EZH2 in oocytes (Figure 4A). In addition, we also tested the potential effect of EZH2 inhibitors on the levels of other PRC2 components including SUZ12 and EED. As shown in Supplementary Figure S5, we did not observe an obvious difference on the levels of SUZ12 and EED with addition of EZH2 inhibitors including DZNep and GSK343, controlled by DMSO. However, the H3K27 trimethylation was decreased with the addition of DZNep or GSK343 in immunofluorescent staining (Figure 4B). Meanwhile, we did not observe an obvious difference for H3 level with or without the treatment of EZH2 inhibitors (Figure 4C). Furthermore, for possible affection of EZH2 inhibitors on H3K9me2 DZNep or GSK343 were applied. We found that DZNep, but not GSK343, could reduce the intensity of H3K9me2 measured by immunofluorescent staining using an anti-H3K9me2 antibody (Supplementary Figure S6), suggesting that EZH2 inhibitor DZNep may reduce the level of H9K9me2. In addition, the rate of GVBD or PB1 extrusion remained not changed during the process of oocyte maturation with or without addition of DZNep or GSK343 (Figure 4D and E). For the karyotype analysis after the treatment by EZH2 inhibitors, we did not observe a statistically significant change in the incidence of aneuploidy. However, when we cultured the oocytes for 14h with addition of GSK343, some oocytes extruded abnormal polar bodies with morphology of giant, small or double polar bodies (Supplementary Figure S7). Interestingly, when we collected these oocytes to perform the chromosome spreading analysis, we found that these polar bodies did show incorrect numbers of chromosomes (data not shown). However, the incidence of these abnormal first polar bodies was very low, and we can only identified one or two abnormal ones from 50 oocytes treated with EZH2 inhibitors. Therefore, we believed that the change of aneuploidy by EZH2 inhibitor treatment is in very low incidence. In addition, we constructed a catalytic inactive EZH2 mutant F667I at the same time. After microinjection of the oocytes with EZH2 mutant F667I mRNA, we found that overexpression of catalytic inactive EZH2 mutant could also lead to chromosome misalignment (Figure 4F and G, mRNA-Control: 15.6 ± 0.98%, $n = 32$; mRNA-EZH2 SET domain mutant: 27 ± 1.3%, $n = 45$, $P < 0.05$). Karyotypic analyses showed a plenty of MII oocytes with aneuploidy after microinjection with EZH2 mutant F667I mRNA (Figure 4H), which were quantified as shown in Figure 4I (mRNA-Control: 15.8 ± 0.68%, $n = 11$; mRNA-EZH2 SET domain mutant: 49.3 ± 3.4%, $n = 15$, $P < 0.05$). Taken together, these results suggested that EZH2 regulation of oocyte meiotic maturation might take an EZH2 methyltransferase-independent mechanism.

EZH2 is required for maintaining the stability of BubR1 in oocytes

Given that SAC proteins regulate oocyte meiotic maturation, a function that overlaps with the depletion or ectopic expression of EZH2 in oocytes. It is reasonable to hypothesize that EZH2 may associate with SAC proteins in oocytes. To this end, we co-stained the oocytes with EZH2 and BubR1 antibodies, the latter is a SAC protein (14). Results indicated that the signals of EZH2 overlapped with those of BubR1 in oocytes (Figure 5A), suggesting that EZH2 is able to encounter BubR1 in the oocytes. Furthermore, the possible mutual affections between EZH2 and BubR1have been examined. Interestingly, when endogenous EZH2 in mouse oocytes was depleted by morpholino the endogenous BubR1 was decreased at Met I stage (Figure 5B, left panel); while when EZH2 was raised by microinjection of EZH2 mRNA into the oocytes, the endogenous BubR1 was increased significantly at Met I stage (Figure 5B, right panel). These data suggested that BubR1 level in oocytes depends on the presence of EZH2. In other words, EZH2 is able to stabilize the endogenous level of BubR1 in oocytes, an important finding that was never reported before.

Since BubR1 is a SAC protein and regulates the timing of first meiosis (14,15), we thus wanted to know whether the EZH2 depletion effect on the acceleration of the PB1 extrusion is mediated by BubR1 in oocytes. To this end, we performed a rescue experiment. By microinjection of in vitro transcribed EZH2 mRNA into the same population of oocytes that were pre-depleted for endogenous EZH2 by MO-EZH2 microinjection for 22 h. After additional blocking for 2 h with the presence of milrinone at the GV stage, oocytes were released in M2 medium allowing re-emergence of BubR1. Western blot analysis showed that BubR1 was restored under the translation of EZH2

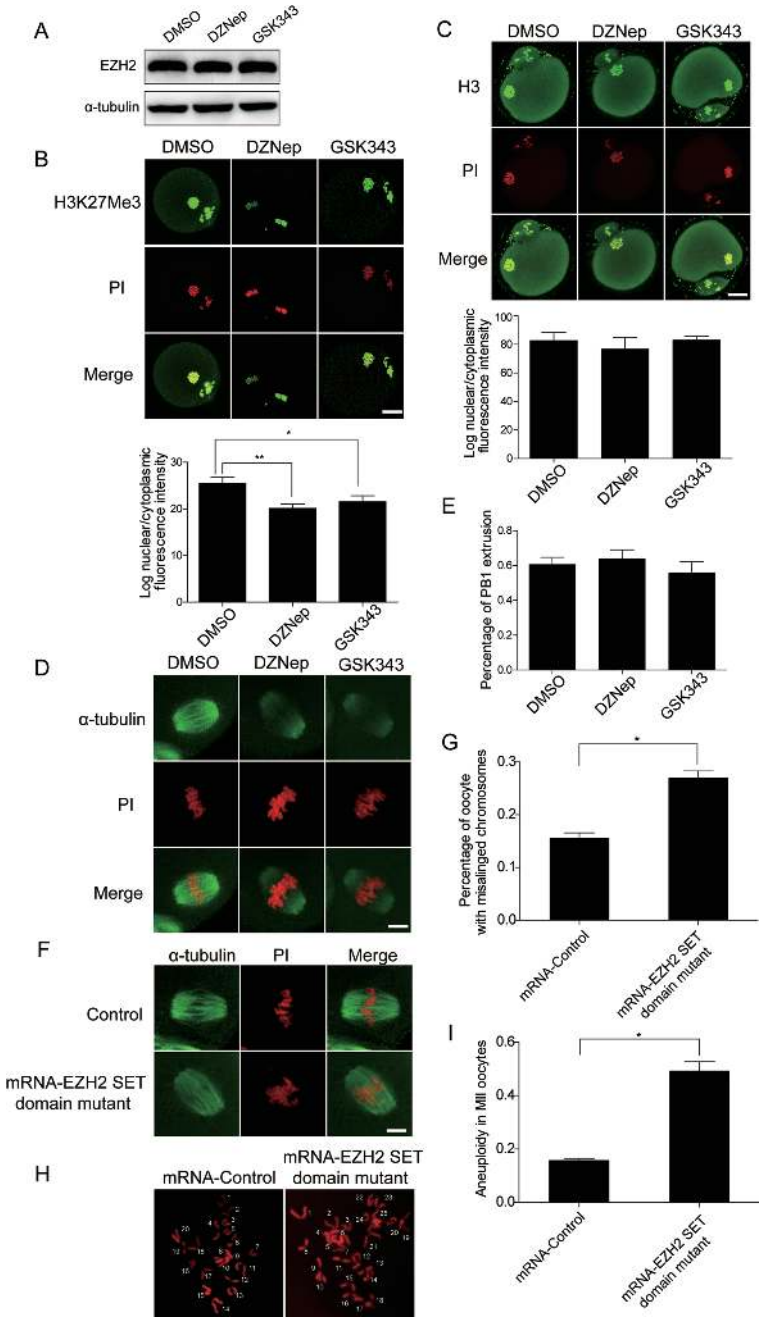

Figure 4. EZH2 methyltransferase activity is not required for oocyte meiotic maturation. (**A**) Oocytes were incubated in M2 medium in the presence of EZH2 inhibitors DZNep or GSK343 for 14 h with DMSO as a control, followed by western blot analysis to detect EZH2 level. (**B**) Upper: representative confocal microscopy images of H3K27me3 staining after treatment of DZNep or GSK343. H3K27me3: green; DNA: red. Scale bar = 20 μm. Lower: quantification of H3K27me3 nuclear fluorescence intensity after DZNep or GSK343 treatment. DNA was stained with PI. Data were shown as mean ± SEM from three independent experiments, $P < 0.05$. The level of tri-methylation of H3K27 was reduced by addition of DZNep or GSK343 in immunofluorescence images. (**C**) Upper: representative confocal microscopy images of H3 staining after treatment of DZNep or GSK343. H3: green; DNA: red. Scale bar = 20 μm. Lower: quantification of H3K27me3 nuclear fluorescent intensity after DZNep or GSK343 treatment. DNA was stained with PI. Data were shown as mean ± SEM from three independent experiments, $P > 0.05$. The level of H3 had no obvious difference by addition of DZNep or GSK343 in immunofluorescent assay. (**D**) Representative confocal microscopy images of oocytes with DZNep or GSK343 treatment. The oocytes presented with a typical barrel-shaped spindle and well-aligned chromosomes on the metaphase plate not only in DZNep or GSK343 treated group but also in the control group. Spindle was recognized by α-tubulin (green) and DNA was recognized by PI (Propidium iodide, red). Scale bar = 4 μm. (**E**) Percentage of the PB1 extrusion of DZNep, GSK343 or DMSO-control treated oocytes. There were no obvious difference between the control or drug treated groups in terms of the PB1 extrusion. Data were presented as mean ± SEM from three independent experiments, $P > 0.05$. (**F**) Overexpression of catalytic inactive EZH2 mutant could also lead to chromosome misalignment. Spindle was recognized by α-tubulin (green) and DNA was recognized by PI (Propidium iodide, red). Scale bar = 4 μm. (**G**) Percentage of oocytes with chromosome misalignment at stage MII was quantified. Data were expressed as mean ± SEM from three independent experiments, $P < 0.05$. (**H**) Chromosome spread in control and EZH2 mutant MII oocytes. Representative fluorescent images of euploid and aneuploid oocytes were shown. (**I**) Percentage of aneuploidy in control and EZH2 mutant oocytes was quantified. Data were expressed as mean ± SEM from three independent experiments, $P < 0.05$.

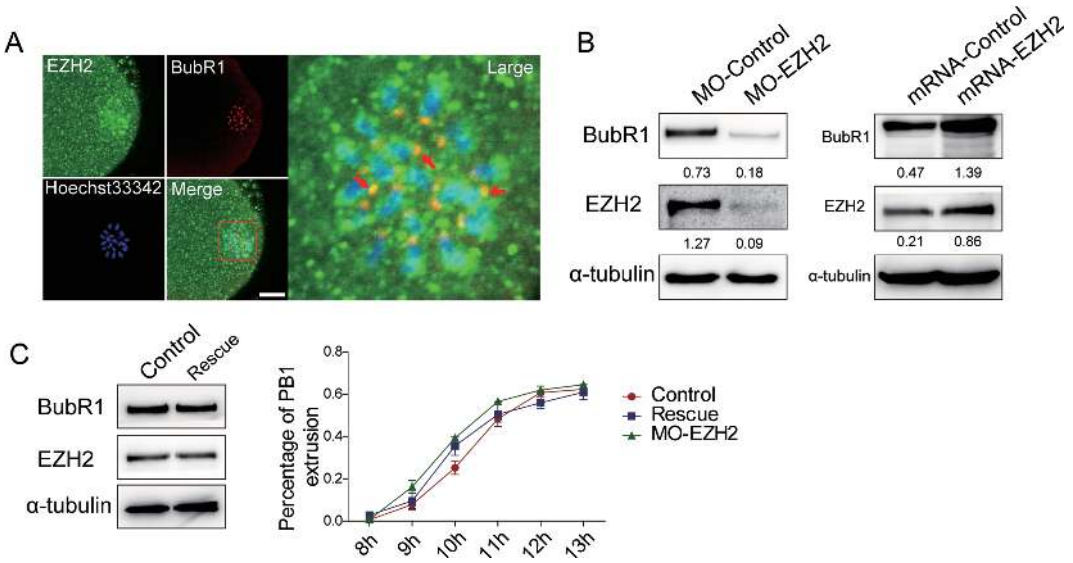

Figure 5. EZH2 is required for maintaining the stability of BubR1 in oocytes. (**A**) EZH2 colocalizes with BubR1 in oocytes. Oocytes were stained with an EZH2 antibody (green), BubR1 was stained with a goat pab (red) and chromosome DNAs were stained by Hoechst 33342. Arrowheads indicated examples of colocalization of EZH2 and BubR1 at kinetochores. Scale bar = 20 μm. (**B**) BubR1 level is dependent of the presence of EZH2. BubR1 protein level was decreased by morpholino depletion of endogenous EZH2 in oocytes (Left panel) and raised in oocytes with microinjection of EZH2 mRNA (right panel). (**C**) EZH2 depletion-induced acceleration of polar body extrusion can be rescued by EZH2 re-expression. Oocytes were microinjected with MO-EZH2 or MO-Control and were cultured in milrinone-M2 medium for 22 h, then mRNA-EZH2 or mRNA-Control was microinjected into the same group of oocytes. After maintaining in milrinone-M2 medium for 2 h to keep the oocytes in GV stage, oocytes were transferred in M2 medium. Left panel: the protein level of BubR1 was rescued to the same level of control. Right panel: no significant change was found for the percentage of PB1extrusion among the control, MO-EZH2 and rescued groups. Data were expressed as mean ± SEM from three independent experiments, $P > 0.05$.

mRNA in oocytes (Figure 5C, left panel), suggesting that BubR1 was rescued by EZH2 at protein level. For functional rescue, the timing for the PB1extrusion showed no significant change among the control, MO-EZH2 and the EZH2 mRNA translated groups (Figure 5C, right panel), strongly indicating that lack of EZH2 caused acceleration of the PB1 extrusion. This effect can be rescued by re-addition of exogenous EZH2. All together, these data convincingly demonstrated that EZH2 regulates oocyte meiotic maturation through maintaining the level of BubR1.

EZH2 forms a molecular complex with BubR1 and PCAF to stabilize BubR1 and regulates oocyte meiotic maturation

In an attempt to examine whether EZH2 may associate with BubR1, a co-IP assay was performed with an EZH2 antibody in oocytes. Indeed, BubR1 was co-IPed endogenously by EZH2 antibody, indicating an interaction between EZH2 and BubR1 in oocytes (Figure 6A). To map which domain of EZH2 may bind to BubR1, we constructed three GST-fusion proteins containing EZH2 individual domains and expressed them in *E. coli* (Figure 6B, upper panel). Due to the difficulties in obtaining large amounts of oocytes for GST pull-down assays, we have to map the binding region between EZH2 and BubR1 in mammalian somatic cells. Using NIH3T3 cell lysates GST pull-down assay showed that BubR1 interacts with EZH2 mainly at the SET domain (aa 610–746) of EZH2, but not the Cys-rich domain (aa 523–609) and the N-terminal domain (aa 1–522) (Figure 6B lower). Accordingly, BubR1 was divided into two fragments and were subcloned into p3×FLAG-CMV-10 expression vector (Figure 6C upper). The two fragments were transfected into NIH3T3 cells individually. Co-IP assay indicated that the N-terminal domain (aa 1–700) but not the C-terminal domain (aa 701–1052) binds to EZH2 (Figure 6C lower). Based on the results above, we constructed two expression vectors: one was Myc-EZH2 (aa 1–609) that contained N-terminal and Cys-rich domains which do not interact with BubR1, and the other one was Myc-EZH2 (aa 610–746) which contained the SET domain that strongly interacts with BubR1. With these expression vectors available, we were able to examine whether the SET domain of EZH2 could raise the level of BubR1 in oocytes. To this end, we microinjected the mRNA of Myc-EZH2 (aa 1–609) and Myc-EZH2 (aa 610–746) into the oocytes. Results showed that the level of BubR1 was upregulated significantly with the expression of Myc-EZH2 (610–746) (Figure 6D, right panel). Reversely, result showed that the level of BubR1 was not obviously changed with the expression of Myc-EZH2 (aa 1–609) (Figure 6D, left panel). These data indicated that it is the SET domain of EZH2 that raise the level of BubR1 in oocytes.

Our laboratory identified that EZH2 is acetylated by PCAF that regulates the stability of EZH2 (22). Intriguingly, it was also reported that BubR1 could be acetylated by PCAF (16). These findings hinted that there may be an inter-relationship among them. Given that EZH2 interacts with both BubR1 and PCAF, it is interesting to hypothesize that EZH2 may form a complex with BubR1 and PCAF. Given that EZH2 colocalizes with BubR1 at kinetochores in oocyte (Figure 5A), it is tempting to examine whether PCAF also colocalizes with BubR1 at the same sites. Results demonstrated that PCAF did colocalize with BubR1 at kinetochores (Figure 6E). This finding suggested that

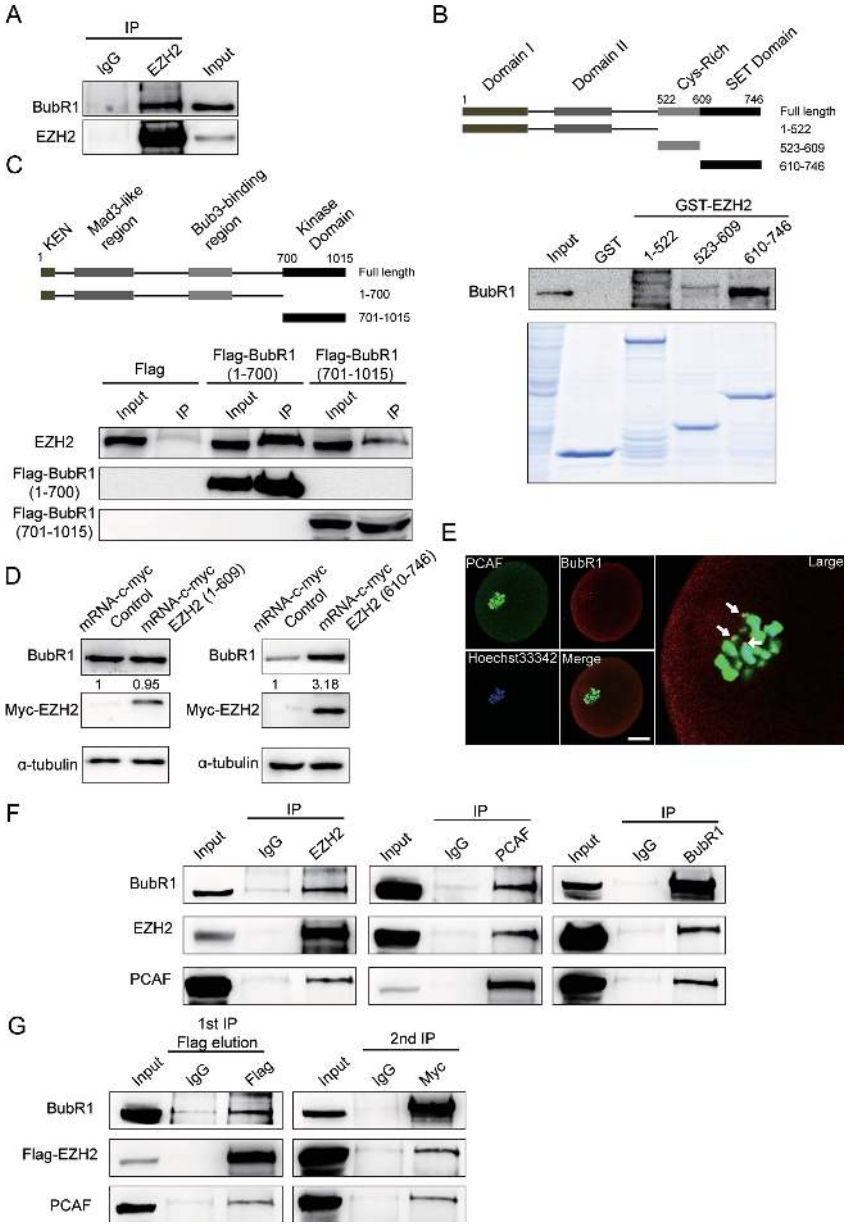

Figure 6. EZH2 stabilizes BubR1 by directly interacting with BubR1 and also forms a complex with BubR1 and PCAF in mouse oocytes. (**A**) EZH2 interacts with BubR1 *in vivo*. BubR1 was co-immunoprecipitated from extracts of approximately 2000 MII oocytes with an EZH2 antibody (lane 2) or with control IgG (lane 1) and 50 MII oocytes were used as input (lane 3). (**B**) EZH2 SET domain interacts with BubR1. Upper panel: domain structure of EZH2. EZH2 domains with aa 1–522, 523–609 and 610–746 were fused with GST and were expressed in *Escherichia coli*. Lower panel: an *in vitro* GST pull-down assay was performed using the above purified GST-EZH2 fragments, and NIH3T3 cell lysates were used as source of BubR1 protein. Protein interaction was detected by western blot analysis with a BubR1 antibody. (**C**) The N-terminus of BubR1 interacts with EZH2. Upper panel: domain structure of BubR1. Lower panel: NIH3T3 cells were transfected with Flag-BubR1 N-terminus (1-700) and Flag-BubR1 kinase domain (701-1052) vectors and then co-IP assays were performed with Flag-M2 beads. Protein interaction was detected by western blot analysis with an EZH2 antibody. Result showed that the N-terminus of BubR1 interacts with EZH2. (**D**) BubR1 protein level is raised by the SET domain of EZH2. Left panel: BubR1 protein level could not be raised by EZH2 N-terminal 1–609. C-myc-EZH2:1-609 mRNA was *in vitro* transcribed and then microinjected into the oocytes for 3 h, followed by transferring to M2 media for 14 h. Experiment was controlled by microinjection of unrelated mRNA. The expression of c-myc-EZH2: 1–609 was detected by a Myc antibody and BubR1 was examined by a BubR1 antibody. Right panel: BubR1 protein level is raised by EZH2 C-terminal 610–746. C-myc-EZH2:610-746 mRNA was *in vitro* transcribed and then microinjected into the oocytes for 3 h, controlled by microinjection of unrelated mRNA. The expression of c-myc-EZH2:610-746 was detected by a Myc antibody and BubR1 was examined by a BubR1 antibody. (**E**) PCAF colocalizes with BubR1 at kinetochores in an oocyte. Oocytes were stained with a PCAF antibody (green), BubR1 was stained with a goat pab (red) and chromosome DNAs were stained by Hoechst 33342. Arrowheads indicated examples of colocalization of PCAF and BubR1 at kinetochores. Scale bar = 20 μm. (**F**) EZH2, BubR1 and PCAF form a complex in mouse oocytes. A panel of co-IP assays using oocyte lysates were performed using EZH2, PCAF or BubR1 antibodies separately and were detected using indicated antibodies. (**G**) EZH2 forms a complex with BubR1 and PCAF in mammalian cells. Total lysates were extracted from NIH3T3 cells co-transfected with Flag-EZH2 and Myc-BubR1 expression vectors, then sequential co-IPs were performed. The first co-IP was performed using FLAG-M2 beads or mouse immunoglobin IgG to immunoprecipitate EZH2. The eluate from the first co-IP was subjected for the second co-IP with an anti-Myc antibody or rabbit IgG to immunoprecipitate BubR1. The detection of immunoprecipitates from the sequential co-IPs was examined by Western blot analysis using indicated antibodies.

EZH2, BubR1 and PCAF are able to colocalize with each other in oocytes, thereby also suggesting that EZH2 may form a complex with BubR1 and PCAF in oocytes. To test this hypothesis, three co-IP assays were performed separately with EZH2, BubR1 and PCAF antibodies in oocytes. Results showed BubR1 and PCAF were co-IPed endogenously by an EZH2 antibody; EZH2 and BubR1 were co-IPed endogenously by a PCAF antibody; and PCAF and EZH2 were co-IPed endogenously with a BubR1 antibody (Figure 6F). These data strongly supported that EZH2 is able form a complex with BubR1 and PCAF in oocytes. To strengthen that these three molecule did form a complex in cells, we performed a two-step sequential co-IP in NIH3T3 cells. NIH3T3 cells were co-transfected with Flag-EZH2 and Myc-BubR1 expression vectors. Cell lysates were subjected for the first co-IP using a Flag antibody and the second co-IP was performed using a Myc antibody. Result showed that EZH2, BubR1 and PCAF do form a molecular complex in mammalian cells (Figure 6G). Taken together, our data suggested that EZH2 maintains BubR1 stability by forming a tripartite complex with BubR1 and PCAF in mouse oocytes, a mechanism that contributes to the control of oocyte meiotic maturation.

DISCUSSION

Maturation of oocytes is a very important step in female reproduction. Given that lack of maternal EZH2 lead to severe growth retardation of neonates (3), we thus attempted to explore the role of EZH2 in the regulation of oocyte meiotic maturation. Here, we identified that EZH2 is required for chromosome accurate alignment and oocyte euploidy by forming a complex with BubR1 but not its methyltransferase activity. It is also for the first time that EZH2 is uncovered to play an important role in the control of oocyte maturation. As shown in the working model, EZH2 maintains the stability of BubR1 by forming a previously unidentified molecular complex with BubR1 and PCAF (Figure 7).

EZH2 catalytic activity is required in pre-implantation embryos, X-chromosome inactivation, stem cell maintenance and cancer progression (3,23–26). In the present study, we find that EZH2 has non-catalytic functions to support meiosis in mouse oocytes. For example, although inhibition of EZH2 by DZNep and GSK343 led to decreased methyltranferase activity, the oocyte meiotic maturation was not affected (Figure 4D and E). At the same time, we found that overexpression of catalytic inactive EZH2 mutant could also lead to chromosome misalignment and aneuploidy (Figure 4F–I), suggesting that the aberrant oocyte development was caused by overexpression of EZH2 but not by its methyltransferase activity. In a separate scenario, Shi *et al*. reported that EZH2 could function as a transcriptional activator through physical interaction with ERα and β-catenin in breast cancer cells independent of its methyltransferase activity (27). Therefore, our findings presented another new paradigm that EZH2 functions independent of its methyltransferase activity.

It was known that SAC and the APC/C function for maintaining the correct chromosome alignment (28,29). BubR1, as a SAC protein, was recognized to be absolutely essential for chromosome alignment and oocyte euploidy (14,15,30). In addition, BubR1 also showed a SAC-independent function that was known to be required for the stabilization of kinetochore-microtubule interactions by counteracting Aurora B phosphorylation through recruitment of PP2A (31–33), and kinetochore-microtubule fibers were diminished upon BubR1 knockdown in the oocytes (14,15). In the present study, our findings strongly suggested that EZH2 is required for chromosome accurate alignment and oocyte euploidy. Furthermore, we also found that kinetochore-microtubule attachments are jeopardized upon EZH2 depletion in oocytes (Figure 2E). Based on the facts that EZH2 interacted with BubR1 in oocytes (Figure 6A–C), we believed that EZH2 is involved in oocyte maturation mainly through its association with the SAC protein BubR1 rather than its methyltransferase activity.

As mentioned before, BubR1 arrests chromosome separation and mitotic progression by inhibiting the activity of APC/C through association with PCAF (16). Anaphase will not be launched unless the inhibition of APC/C is released so that BubR1 could modulate timing of mi-

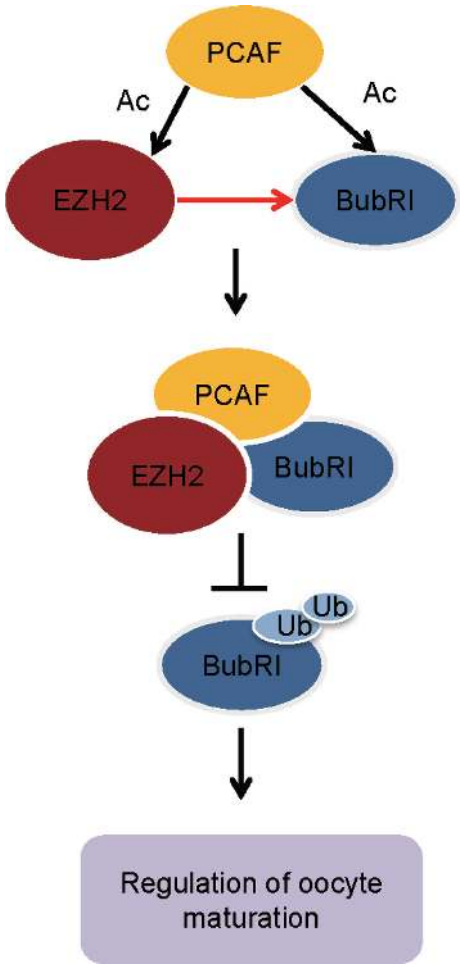

Figure 7. A working model depicting how EZH2 regulates oocyte meiotic maturation. This model is based on the previous findings and the identification of EZH2 interaction with BubR1 in mouse oocytes. In this model EZH2 could controls the oocyte meiotic maturation in mice by preventing the degradation of BubR1 thought interactions with PCAF in a new way.

tosis (34). Interestingly, we previously found that PCAF could acetylate EZH2 and stabilize it (22). We therefore examined whether EZH2, BubR1 and PCAF might associate with each other in oocytes. Intriguingly, a sequential co-immunoprecipitation experiment precisely proved that these three molecules could form a complex in cells (Figure 6E–G). We then developed a model, through which EZH2 could stabilize BubR1 and prevents its degradation thought interaction with PCAF. Due to the technical limitation, however, it is very difficult to reproduce the sequential co-immunoprecipitation experiment for direct molecular interactions of these three molecules in mouse oocytes. Fortunately, individual co-immunoprecipitations using EZH2, BubR1 and PCAF antibodies separately did precipitate the corresponding molecule in the mouse oocytes, indicating that these three molecules associate with each other and may cooperate to regulate the oocyte meiotic maturation in the mouse oocytes. Apparently EZH2 regulation of oocyte meiotic maturation simply opened a new window, but mysteries still remain for future investigations on the role of EZH2 in meiosis of oocyte maturation, and on the accurate control of spindle assembly in mammalian somatic cells. Abnormal function of EZH2 may cause reproductively related disorders in female mice and would possibly lead to infertility in women. However, the precise role of EZH2 in female mouse reproduction might be explored by use of oocyte specific knockout mice.

In summary, in this report we have defined a new function of EZH2 in female mouse reproduction by demonstrating that EZH2 is required for oocyte meiotic maturation. EZH2 maintains the chromosome accurate alignment and oocyte euploidy through controlling the amount of BubR1 in oocytes. EZH2–BubR1 interaction represents a new mechanism underlying inhibition of BubR1 degradation during meiosis of mouse oocytes.

SUPPLEMENTARY DATA

Supplementary Data are available at NAR Online.

FUNDING

Ministry of Science and Technology of China [2015CB553906, 2013CB910501]; National Natural Science Foundation of China [81230051, 81472734, 31170711, 81321003, 30830048]; Beijing Natural Science Foundation [7120002]; 111 Project of the Ministry of Education; Peking University [BMU20120314, BMU20130364]; Leading Academic Discipline Project of Beijing Education Bureau (to H.Z.).

Conflict of interest statement. None declared.

REFERENCES

1. Simon,J.A. and Kingston,R.E. (2009) Mechanisms of polycomb gene silencing: knowns and unknowns. *Nat. Rev. Mol. Cell Biol.*, **10**, 697–708.
2. Cao,R., Wang,L., Wang,H., Xia,L., Erdjument-Bromage,H., Tempst,P., Jones,R.S. and Zhang,Y. (2002) Role of histone H3 lysine 27 methylation in Polycomb-group silencing. *Science*, **298**, 1039–1043.
3. Erhardt,S. (2003) Consequences of the depletion of zygotic and embryonic enhancer of zeste 2 during preimplantation mouse development. *Development*, **130**, 4235–4248.
4. Huang,X.J., Wang,X., Ma,X., Sun,S.C., Zhou,X., Zhu,C. and Liu,H. (2014) EZH2 is essential for development of mouse preimplantation embryos. *Reprod. Fertil. Dev.*, **26**, 1166–1175.
5. Grossniklaus,U., Vielle-Calzada,J.-P., Hoeppner,M.A. and Gagliano,W.B. (1998) Maternal control of embryogenesis by MEDEA, a polycomb group gene in Arabidopsis. *Science*, **280**, 446–450.
6. Furuno,N., Nishizawa,M., Okazaki,K., Tanaka,H., Iwashita,J., Nakajo,N., Ogawa,Y. and Sagata,N. (1994) Suppression of DNA-replication via mos function during meiotic divisions in Xenopus-Oocytes. *EMBO J.*, **13**, 2399–2410.
7. Petronczki,M., Siomos,M.F. and Nasmyth,K. (2003) Un Ménage à Quatre:the molecular biology of chromosome segregation in meiosis. *Cell*, **113**, 423–440.
8. Menasha,J., Levy,B., Hirschhorn,K. and Kardon,N.B. (2005) Incidence and spectrum of chromosome abnormalities in spontaneous abortions: New insights from a 12-year study. *Genet. Med.*, **7**, 251–263.
9. Nagaoka,S.I., Hassold,T.J. and Hunt,P.A. (2012) Human aneuploidy: mechanisms and new insights into an age-old problem. *Nat. Rev. Genet.*, **13**, 493–504.
10. Wang,Q. and Sun,Q.Y. (2007) Evaluation of oocyte quality: morphological, cellular and molecular predictors. *Reprod. Fertil. Dev.*, **19**, 1–12.
11. Musacchio,A. and Salmon,E.D. (2007) The spindle-assembly checkpoint in space and time. *Nat. Rev. Mol. Cell Biol.*, **8**, 379–393.
12. Peters,J.M. (2006) The anaphase promoting complex/cyclosome: a machine designed to destroy. *Nat. Rev. Mol. Cell Biol.*, **7**, 644–656.
13. London,N. and Biggins,S. (2014) Signalling dynamics in the spindle checkpoint response. *Nat. Rev. Mol. Cell Biol.*, **15**, 736–747.
14. Wei,L., Liang,X.W., Zhang,Q.H., Li,M., Yuan,J., Li,S., Sun,S.C., Ouyang,Y.C., Schatten,H. and Sun,Q.Y. (2010) BubR1 is a spindle assembly checkpoint protein regulating meiotic cell cycle progression of mouse oocyte. *Cell Cycle*, **9**, 1112–1121.
15. Touati,S.A., Buffin,E., Cladiere,D., Hached,K., Rachez,C., van Deursen,J.M. and Wassmann,K. (2015) Mouse oocytes depend on BubR1 for proper chromosome segregation but not for prophase I arrest. *Nat. Commun.*, **6**, 6946.
16. Choi,E., Choe,H., Min,J., Choi,J.Y., Kim,J. and Lee,H. (2009) BubR1 acetylation at prometaphase is required for modulating APC/C activity and timing of mitosis. *EMBO J.*, **28**, 2077–2089.
17. Yu,Y., Wu,J., Wang,Y., Zhao,T., Ma,B., Liu,Y., Fang,W., Zhu,W.G. and Zhang,H. (2012) Kindlin 2 forms a transcriptional complex with beta-catenin and TCF4 to enhance Wnt signalling. *EMBO Rep.*, **13**, 750–758.
18. Rieder,C.L. (1981) The structure of the cold-stable kinetochore fiber in metaphase PtK1 cells. *Chromosoma*, **84**, 145–158.
19. Tan,J., Yang,X., Zhuang,L., Jiang,X., Chen,W., Lee,P.L., Karuturi,R.K., Tan,P.B., Liu,E.T. and Yu,Q. (2007) Pharmacologic disruption of Polycomb-repressive complex 2-mediated gene repression selectively induces apoptosis in cancer cells. *Genes Dev.*, **21**, 1050–1063.
20. Amatangelo,M., Garipov,A., Li,H., Conejo-Garcia,J.R., Speicher,D. and Zhang,R. (2013) Three-dimensional culture sensitizes epithelial ovarian cancer cells to EZH2 methyltransferase inhibition. *Cell Cycle*, **12**, 2113–2119.
21. Béguelin,W., Popovic,R., Teater,M., Jiang,Y., Bunting,K.L., Rosen,M., Shen,H., Yang,S.N., Wang,L. and Ezponda,T. (2013) EZH2 is required for germinal center formation and somatic EZH2 mutations promote lymphoid transformation. *Cancer Cell*, **23**, 677–692.
22. Wan,J., Zhan,J., Li,S., Ma,J., Xu,W., Liu,C., Xue,X., Xie,Y., Fang,W., Chin,Y.E. *et al.* (2015) PCAF-primed EZH2 acetylation regulates its stability and promotes lung adenocarcinoma progression. *Nucleic Acids Res.*, **43**, 3591–3604.
23. van der Vlag,J. and Otte,A.P. (1999) Transcriptional repression mediated by the human polycomb-group protein EED involves histone deacetylation. *Nat. Genet.*, **23**, 474–478.
24. Plath,K., Fang,J., Mlynarczyk-Evans,S.K., Cao,R., Worringer,K.A., Wang,H., Cecile,C., Otte,A.P., Panning,B. and Zhang,Y. (2003) Role of histone H3 lysine 27 methylation in X inactivation. *Science*, **300**, 131–135.
25. Lee,T.I., Jenner,R.G., Boyer,L.A., Guenther,M.G., Levine,S.S., Kumar,R.M., Chevalier,B., Johnstone,S.E., Cole,M.F. and

Isono,K.-i. (2006) Control of developmental regulators by Polycomb in human embryonic stem cells. *Cell*, **125**, 301–313.
26. Simon,J.A. and Lange,C.A. (2008) Roles of the EZH2 histone methyltransferase in cancer epigenetics. *Mutat. Res.*, **647**, 21–29.
27. Shi,B., Liang,J., Yang,X., Wang,Y., Zhao,Y., Wu,H., Sun,L., Zhang,Y., Chen,Y., Li,R. *et al.* (2007) EZH2 oncogenic activity in castration-resistant prostate cancer cells is polycomb-independent. *Mol. Cell. Biol.*, **338**, 1465–1469.
28. Wang,L., Lu,A., Zhou,H.-X., Sun,R., Zhao,J., Zhou,C.-J., Shen,J.-P., Wu,S.-N. and Liang,C.-G. (2013) Casein kinase 1 alpha regulates chromosome congression and separation during mouse oocyte meiotic maturation and early embryo development. *PLoS One*, **8**, e63173.
29. Homer,H. (2011) New insights into the genetic regulation of homologue disjunction in mammalian oocytes. *Cytogenet. Genome Res.*, **133**, 209–222.
30. Homer,H., Gui,L. and Carroll,J. (2009) A spindle assembly checkpoint protein functions in prophase I arrest and prometaphase progression. *Science*, **326**, 991–994.
31. Kruse,T., Zhang,G., Larsen,M.S., Lischetti,T., Streicher,W., Kragh Nielsen,T., Bjorn,S.P. and Nilsson,J. (2013) Direct binding between BubR1 and B56-PP2A phosphatase complexes regulate mitotic progression. *J. Cell Sci.*, **126**, 1086–1092.
32. Ditchfield,C., Johnson,V.L., Tighe,A., Ellston,R., Haworth,C., Johnson,T., Mortlock,A., Keen,N. and Taylor,S.S. (2003) Aurora B couples chromosome alignment with anaphase by targeting BubR1, Mad2, and Cenp-E to kinetochores. *J. Cell Biol.*, **161**, 267–280.
33. Xu,P., Raetz,E.A., Kitagawa,M., Virshup,D.M. and Lee,S.H. (2013) BUBR1 recruits PP2A via the B56 family of targeting subunits to promote chromosome congression. *Biol. Open*, **2**, 479–486.
34. Kapanidou,M., Lee,S. and Bolanos-Garcia,V.M. (2015) BubR1 kinase: protection against aneuploidy and premature aging. *Trends Mol. Med.*, **21**, 364–372.